Exciton-phonon scattering and photoexcitation dynamics in *J*-aggregate microcavities

Paolo Michetti*
Dipartimento di Fisica, Università di Pisa, Largo Bruno Pontecorvo 3, 56127 Pisa, Italy

Giuseppe C. La Rocca
Scuola Normale Superiore and CNISM, Piazza dei Cavalieri 7, 56126 Pisa, Italy

(Received 16 October 2008; revised manuscript received 30 December 2008; published 27 January 2009)

We have developed a model accounting for the photoexcitation dynamics and the photoluminescence of strongly coupled *J*-aggregate microcavities. Our model is based on a description of the *J*-aggregate film as a disordered Frenkel exciton system, in which relaxation occurs due to the presence of a thermal bath of molecular vibrations. In a strongly coupled microcavity exciton polaritons are formed, mixing super-radiant excitons and cavity photons. The calculation of the microcavity steady-state photoluminescence, following a cw nonresonant pumping, is carried out. The experimental photoluminescence intensity ratio between upper and lower polariton branches is accurately reproduced. In particular, both thermal activation of the photoluminescence intensity ratio and its Rabi splitting dependence are a consequence of the bottleneck in the relaxation, occurring at the bottom of the excitonic reservoir. The effects due to radiative channels of decay of excitons and to the presence of a particular set of discrete optical molecular vibrations active in relaxation processes are investigated.

DOI: 10.1103/PhysRevB.79.035325 PACS number(s): 78.66.Qn, 71.36.+c, 78.20.Bh, 71.35.Aa

I. INTRODUCTION

Strong coupling in solid-state microcavities (MCs) has been exhaustively studied in inorganic quantum well devices.[1] In these structures Wannier excitons and photon cavity modes are mixed in coherent excitations called polaritons. A number of interesting phenomena due to the mixed nature of such eigenstates, such as the parametric processes[2] and nonequilibrium polariton condensation,[3] were revealed.

On the other hand, organic strongly coupled MCs have been developed since 1998,[4] by using different kinds of optically active organic layers, among which the cyanine dye *J*-aggregate films are probably the most typical. Organic materials possess Frenkel excitons instead of Wannier ones with large binding energy and oscillator strength. Because of this, organic MCs allow obtaining values of the Rabi splitting up to 300 meV (Ref. 5) and offer the possibility of easily observing polaritons at room temperature.[6] Electroluminescence was demonstrated in a *J* aggregate strongly coupled microcavity light-emitting diode (LED) (Ref. 7) at room temperature. Peculiar molecular phenomena, such as the observation of strongly coupled vibronic replicas, have also been demonstrated.[8,9] A detailed review about organic MCs can be found in Refs. 10 and 11.

The nature of polaritons in disordered organic MCs has been addressed from the theoretical point of view,[12–15] showing the coexistence of delocalized and partially localized polaritons. The possible interaction with molecular vibrations was discussed,[16,17] the effect of anisotropy in organic crystal was characterized,[18] as well as the possible occurrence of nonlinear phenomena[19] for high density of polaritons.

We believe that, as in the case of inorganic MCs, theoretical efforts toward a qualitative—but also quantitative—understanding of the relaxation processes in organic MCs dynamics are an essential support to the work of experimental teams involved in the study of organic microcavities, which are in principle able to give rise to a rich variety of phenomena, similar to what is obtained with their inorganic counterpart and more, thanks to the infinite possibilities of organic chemistry. A recent model described the dynamics of a *J*-aggregate MC due to the strong coupling of polaritons with optical molecular vibrations[20] through the application of a quantum kinetic theory. Our approach,[17] even though restricted to a rate equation description of the relaxation processes, allows for a more flexible and complete description of the physical system at hand, accounting for the photoluminescence (PL) of a two-dimensional (2D) MC starting from an accurate description of the bare active material (the *J*-aggregate film). Besides, we are also able to perform time-dependent simulations of *J*-aggregate microcavity photoluminescence[21] and estimate their radiative decay time in linear pumping regime. In particular, we here extend our model, which includes the presence of a large number of weakly coupled excitons, considering the occurrence of a radiative relaxation channel from such excitons to the cavity polaritons, as first suggested in Ref. 22. We also include the effects on the polariton relaxation due to the presence of a discrete spectrum of molecular vibrations, as in Ref. 20, which however are—here—supposed to scatter weakly with the electronic excitations without taking part directly in the cavity-polariton formation.

II. MODEL

A *J* aggregate can be thought as a chain of N_d dye molecules linked by electrostatic interactions. Its excitations are described by the Frenkel Hamiltonian,

$$H = \sum_{i}^{N_d} E_i b_i^\dagger b_i + \sum_{i \neq j}^{N_d} V_{i,j}(b_i^\dagger b_j + b_j^\dagger b_i), \tag{1}$$

where $b_i^\dagger$ are the monomer exciton creation operators, corresponding to Gaussian-distributed energies E_i, with standard

deviation σ, to account for static disorder. The hopping term is given by $V_{i,j}=-J/|i-j|^3$, where $J>0$ is the nearest-neighbor coupling strength. The eigenstates are found by direct diagonalization of the Frenkel Hamiltonian and are described by the operators $B_\alpha^\dagger=\Sigma_i c_i^{(\alpha)} b_i^\dagger$, where c_i^α is the coefficient of the αth exciton on the ith monomer. The oscillator strength of each state is given by $F_\alpha=|\Sigma_i c_i^{(\alpha)}|^2$, with $\Sigma_\alpha F_\alpha=N_d$, having the molecules equal the transition dipole and being the wavelength much greater than the aggregate length. The excitations are delocalized Frenkel excitons with an energy dispersion curve called the J band, where most part of the aggregate oscillator strength is concentrated on the super-radiant bottom states.[23] Higher-energy excitons very weakly couple with light. While the hopping term determines the formation of the J band, static disorder gives rise to a low-energy tail in the exciton density of states (DOS), corresponding to partially localized, inhomogeneously broadened, and super-radiant eigenstates responsible for the film luminescence and, in MCs, of the strong light-matter coupling.

Delocalized polaritons are the result of the strong light-matter interaction between such super-radiant excitons localized on each aggregate and the photon cavity modes ideally extended over the whole structure. To treat the MC case, we include a model polariton wave function of wave vector k, linking the J aggregate excitons into the polariton states.[17] The total exciton and photon fraction $C_k^{(\mathrm{ex})}, C_k^{(\mathrm{ph})}$ and the polariton dispersion curve $E_{U,L}(k)$ are given by the usual two coupled oscillator model. The modulus of the exciton coefficients $\phi_{\alpha,I}^{(k)}$, describing how each exciton α of Ith aggregate participates in the polariton states, is the only relevant quantity entering our model. We consider the polaritons to be extended with equal degree on each one of the N_{agg} aggregates and make the assumption that the weight of each exciton in the polariton states is proportional to its oscillator strength, so that $|\phi_{\alpha,I}^{(k)}|=\sqrt{F_\alpha/N_d}$.

In organic microcavities, the strong-coupling region, where polaritons form, is typically extended until about $q_{\max}=10^5$ cm^{-1}, where the Bragg mirrors stop band starts to fail, or is also more restricted by inhomogeneous disorder.[12,15] Therefore the excitation spectrum is composed—besides polaritons—of a number of uncoupled molecular excitons that form an excitonic reservoir (ER) (Refs. 12, 15, and 16) as shown in Fig. 1. The excitonic part of the polaritons is formed by a Bloch sum, with $q<q_{\max}$, made from the super-radiant molecular excitons of the J aggregates, while the ER is composed by uncoupled super-radiant excitons from the remaining part of the Brillouin zone plus a number of higher-energy "dark" excitons. We note that the ratio between polaritons and uncoupled excitons of the ER can be of the order of 10^{-3} or less.

The dynamics of the system is described by rate equations for the population $f_i(t)$ of the state i, including the scattering rates, due to a weak linear exciton-phonon coupling, among all the kinds of particles present in the system which have a non-null exciton component. Dealing with a 2D microcavity, we assume isotropic conditions, in which the polariton population only depends on the modulus of the wave vector, in order to reduce the dimensionality of the problem. We consider localized vibrations that can be due to the monomer

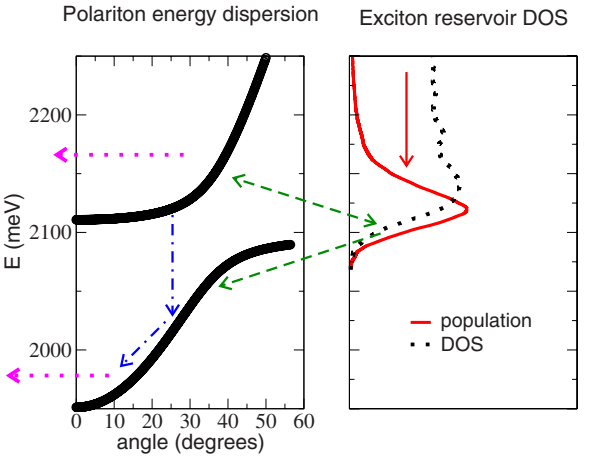

FIG. 1. (Color online) On the left polariton dispersion curves for $\Delta=80$ meV, on the right the exciton reservoir DOS (dotted line), and steady-state population (continuous line) are represented. The possible scattering mechanisms are sketched out: exciton to exciton (continuous arrow), exciton to/from polariton (dashed arrow), polariton to polariton (dotted-dashed arrow), polariton radiative decay (dotted arrow).

itself or to the local environment located on each chain site with a continuous spectrum, a choice that follows literature reports[24,25] on J-aggregate simulations. We will address this model as the continuous spectrum of vibration (CSV) model. We also extend the model to account for a series of discrete optical vibrations in what we will refer to as the discrete vibrations model (DV model); such specific modes can be of particular relevance when their energy is nearly resonant with the Rabi splitting.[20,22] In particular, the DV model includes a continuum of vibrations for energy below $E_{\mathrm{CSM}}=25$ meV and two discrete molecular vibrations of $E_1=40$ meV and $E_2=75$ meV, with an exciton-phonon coupling factor $g_1=0.4$ and $g_2=0.5$, respectively. The values of the molecular vibrations are chosen following the Raman experiments on J-aggregate films, as reported in Ref. 20.

The scattering rates from the state i to i', which can either be an exciton $i=n=(\alpha,I)$, the αth exciton of the Ith aggregate, or a delocalized polariton of wave vector k, can be expressed in a unique compact notation. If we consider the interaction with a continuous spectrum of vibrations, for which the vibrational DOS is nonzero for any energy difference $\Delta E=E_{i'}-E_i$ between final and initial states, we adopt the following expression:

$$W_{i',i}=W_0\Xi_{i,i'}(N_{|\Delta E|}+\Theta_{(\Delta E)})\left(\frac{|\Delta E|}{J}\right)^p, \qquad (2)$$

where W_0 and p are parameters related to the exciton-phonon interaction energy and to the shape of the vibration spectrum, $N_{|\Delta E|}$ is the Bose-Einstein occupation factor and $\Theta_{(\Delta E)}$ is the step function. If we instead consider the interaction with a molecular vibration of discrete energy E_{vib}, we obtain

$$W_{i',i}=\frac{2\pi g^2 E_{\mathrm{vib}}^2}{\hbar}\Xi_{i,i'}(N_{|\Delta E|}+\Theta_{(\Delta E)})\delta(|\Delta E|-E_{\mathrm{vib}}), \qquad (3)$$

where $\delta(E)$ is the Dirac delta and g is the exciton-phonon coupling parameter for the vibration of energy E_{vib}. What distinguishes the different processes is the overlap factor $\Xi_{i,i'}$. In fact, the emission or absorption of localized vibrations promotes the scattering among states that have an exciton participation on the same molecular site. Therefore the factor $\Xi_{i,i'}$ takes into account the partial exciton nature of polaritons and their delocalized nature and is proportional to an excitonic overlap factor I obtained by carrying out the sum of the excitonic participation of the initial and final states on each molecular site. The overlap factor is one of the following:

$$\Xi_{n,n'} = \delta_{I,I'} I_{\alpha,\alpha'}, \tag{4}$$

$$\Xi_{k,n'} = \frac{D(k)|C_k^{(\mathrm{ex})}|^2}{N_{\mathrm{agg}}} I_{n'}^{(\mathrm{ex\text{-}pol})}, \tag{5}$$

$$\Xi_{n',k} = \frac{|C_k^{(\mathrm{ex})}|^2}{N_{\mathrm{agg}}} I_{n'}^{(\mathrm{ex\text{-}pol})}, \tag{6}$$

$$\Xi_{k',k} = \frac{D(k')|C_{k'}^{(\mathrm{ex})}|^2 |C_k^{(\mathrm{ex})}|^2}{N_{\mathrm{agg}}^2} I^{(p\text{-}p)}, \tag{7}$$

respectively, in the case of scattering from an exciton to another exciton ($i=n$, $i'=n'$), where $I_{\alpha,\alpha'}$ is the excitonic overlap factor; or for the scattering from an exciton n' to a polariton k, with $I_{n'}^{\mathrm{ex\text{-}pol}}$ as their excitonic overlap factor, and $D(k)$ as the number of states corresponding, in the inverse space grid, to the polariton variable of modulus wave vector k; or when describing the opposite process ($i=k$, $i'=n'$); or in the latter case of scattering between two polaritons, where $I^{(p\text{-}p)}$ is an excitonic overlap factor between polaritons (the derivation of the rates can be found in Ref. 17).

We also add a radiative channel of decay from the ER to the polaritons, accounting for the presence in the MC of a fraction of excitons weakly coupled with light. In fact, inside a strongly coupled cavity a fraction of weakly coupled excitons can decay radiatively pumping the photonic part of polaritons.[22] We model the spontaneous emission of polaritons from the ER similar to the bare film photoluminescence times a switching factor β,

$$W_{k,\alpha}^{\mathrm{rad}} = \beta \gamma_\alpha \frac{D(k)|C_k^{(\mathrm{ph})}|^2 g_\alpha(E_k)}{\sum_{k'} D(k')|C_{k'}^{(\mathrm{ph})}|^2 g_\alpha(E_{k'})}. \tag{8}$$

The contribution of the α excitons is proportional to the bare exciton luminescence ratio γ_α, the transfer matches energy conservation, while the normalization is chosen to obtain a net exciton radiative decay toward polaritons of β times the spontaneous emission (γ_α). g_α is a Lorentzian shape broadening function, where the energy uncertainty is given by the finite particle lifetime.

The damping rate of polaritons due to photon escape through the cavity mirrors is given by $\Gamma_i = |C_i^{(\mathrm{ph})}|^2/\tau$, where typically $\tau=35$ fs. For the upper and lower polaritons (UP LPs), we consider the reciprocal space up to $q_{\max}=9 \times 10^4$ cm^{-1} discretized in a grid of 280 points. The effect of the inhomogeneous disorder is taken into account averaging the scattering rates over an ensemble of 10^3 J aggregates, each having $N_d=100$ monomers. The dye's hopping energy is fixed at $J=75$ meV and the dye spontaneous emission lifetime is $\gamma_0=0.33$ ns^{-1}, while the parameters $\sigma=0.54J$, $p=0.8$, and $W_0=3.2J/\hbar$ have been fixed in order to obtain the best fit to the bare J-aggregate film absorption and emission features.[17]

III. PHOTOLUMINESCENCE SIMULATION

A. Continuous spectrum of vibrations

Solving the rate equations for the J-aggregate microcavity with the same procedure described in Ref. 17, we obtain the polariton steady-state population, from which we calculate the angle-resolved photoluminescence, by imposing the conservation of energy and in-plane momentum between cavity polaritons and external photons. For both the CSV and the DV models, we draw the indication that the major part of the population is frozen on the ER. The origin of this bottleneck is due essentially to three reasons. First, the small number of polariton states with respect to the ER ones; second, the interaction between a localized vibration and a polariton is reduced by the delocalized and mixed nature of exciton polaritons; in fact the scattering rates scale as $1/N_{\mathrm{coher}}$, where N_{coher} is the number of molecular sites over which the polariton is delocalized. Third is the small photon lifetime, due to the low-quality factor of organic MCs. The photoluminescence can be thought of as the result of the escape through the cavity mirrors of a particle, following the previous scattering on the polariton branches from the ER, with the absorption or emission of a vibrational quantum.

In Fig. 1 we draw a sketch of the excited states on a J-aggregate microcavity and of the possible scattering processes following nonresonant pumping. In particular, we stress that the relaxation inside a J aggregate is faster than ER to polariton scattering and leads to a steady-state population (shown in the right figure in continuous line), from which polariton pumping occurs. The ER DOS is inhomogeneously broadened by static disorder and the ER steady-state population is similar to that of a noncavity sample. We note here that the average difference between the energy of the steady-state population and the film absorption maximum results to be about $\varepsilon=15$ meV.

An experimentally accessible parameter used to analyze the effectiveness of relaxation in organic microcavities is the photoluminescence intensity ratio $C=\mathrm{UPPL}/\mathrm{LPPL}$ recorded at resonance angle, where polariton branches are half matter and half light, and their energy distance from the exciton resonance is half the Rabi splitting ($\Delta/2$). We focus on the temperature dependence of the C ratio between 50 and 300 K for a MC with a Rabi splitting of $\Delta=130$ meV, shown in Fig. 2, and compare it with the experimental result reported by Lidzey and co-workers.[26] With $\beta^{\mathrm{rad}}=0$ the C ratio shows a smooth thermal activation, but it is difficult to get any UP PL at low temperature. This is consistent with the fact that UP PL follows the absorption of a vibrational quantum from a particle at the bottom of the ER and therefore is proportional to the number of vibrations (varying as a Boltzmann

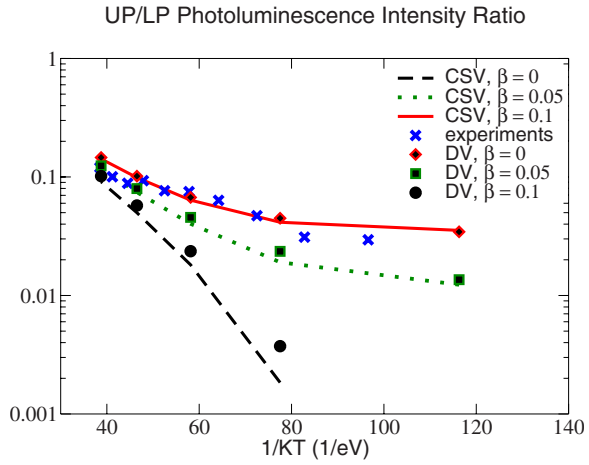

FIG. 2. (Color online) The C ratio as a function of temperature for a MC with $\Delta=130$ meV. The experimental results from Ref. 26 ("x's") are compared with simulations with increasing importance of the radiative channel $\beta^{\mathrm{rad}}=0$, 0.05, and 0.1 for both the model with continuous spectrum of vibrations and the DV model.

factor). Turning on the radiative channel ($\beta^{\mathrm{rad}}>0$), it being independent of temperature, we obtain a low-temperature saturation of the UP PL and the C ratio exhibits a plateau as experimentally found.[26,27] The experimental data are well reproduced and stay between the simulations with $\beta^{\mathrm{rad}}=0.05$ and 0.1.

We also show in Fig. 3 the simulation of the C ratio as a function of the Rabi splitting in comparison with experimental data from Ref. 20. Increasing the Rabi splitting value reduces the probability for a particle in the ER to be scattered on the UP branch because such process would need the absorption of a vibration of greater energy from the thermal bath. The data therefore roughly follow a Boltzmann factor $e^{-\Delta/2K_bT}$ shown for comparison, where $\Delta/2$ corresponds—at resonance angle—to the energy separation from the ER bottom and the UP and LP states. With a continuous vibrational spectrum, we observe the smooth Boltzmann behavior, while

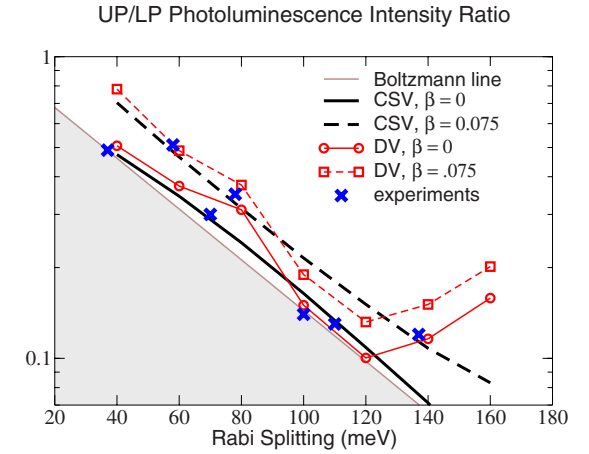

FIG. 3. (Color online) The C ratio as function of the Rabi splitting for microcavities with $\beta=0$ and 0.075, for the models with continuous and discrete spectrum of vibrations. The calculation is compared with the experimental data in "x's" (Ref. 20).

the inclusion of the radiative channel rigidly shifts the C ratio toward higher values. The experimental data (blue x symbols) stay in between the simulation performed without the radiative channel $\beta=0$ and the simulation with the radiative process turned on with $\beta=0.075$.

B. Model with discrete vibrations

The temperature dependence of the C ratio shown in Fig. 2 is largely unaffected by the introduction of the discrete spectrum of vibration and the same considerations as for the CSV case still apply. If we instead consider the Rabi splitting dependence, the inclusion of discrete energy vibrations leads to the fluctuation of the C ratio and to a deviation from the smooth Boltzmann-type behavior. In particular the DV model reproduces the drop in the C factor between 80 to 100 meV associated with $\Delta/2\approx 40$ meV and the activation of the UP depletion toward the ER bottom with emission of a vibrational quantum and permits to obtain a better fit of experimental data. We believe that the agreement we obtain with the available data as shown in Fig. 3 is of comparable quality to that obtained by Chovan *et al.*[20] Of course, this is not to say that the phonon strong-coupling approach they consider is immaterial. It is plausible that also in J-aggregate microcavities exciton and molecular vibrations may interact strongly leading to nonperturbative effects[8,9,28] such as, in particular, the formation of cavity polaritons with the concomitant participation of optical phonon, exciton, and cavity photon modes: a phenomenon which has also been considered in bulk semiconductors (see the concept of "phonoriton"[29]). It remains to be seen, however, whether there is as yet a compelling experimental evidence for the occurrence of such a phonon strong coupling in J-aggregate microcavities, the photoluminescence of which is here considered.

Apart from the particular choice of the definite energy vibrations we made in the DV model ($E_{\mathrm{CSM}}=25$ meV, $E_1=40$ meV, $E_2=75$ meV), we also tested different sets of optical vibrations in order to understand their effects on the C ratio as a function of the Rabi splitting. In general it is not possible to completely distinguish the individual effects of each one of E_{CSM}, E_1, and E_2; however we are able to identify some trends.

First we analyze the role of optical vibration E_2 by increasing it from 65 to 85 meV. As shown in Fig. 4 a minimum is observed at different Δ for different values of E_2. The motivation is that the ER to LP scattering rate is in resonance when $E_{\mathrm{ER}}-E_{\mathrm{LP}}\approx E_2$, with E_{ER} averaged on the steady-state population of the exciton reservoir. When the process is in full resonance, we expect a minimum of the C factor, as it is evidenced in Fig. 4. Following this rule, we expect the minimum to be located in $\Delta_{\mathrm{min}}=2(E_2-\varepsilon)$. Because of the different position of Δ_{min}, when ER to LP scattering is maximum, for small Rabi splitting the C factor decreases with E_2, while we find the opposite behavior for Δ greater than 100 meV. As we will see, the occurrence of the C minimum depends on the absence of higher-energy vibrations active in relaxation processes, not included here.

We now focus on the role of the low-energy vibrations. Initially we modify the DV model including the single vibra-

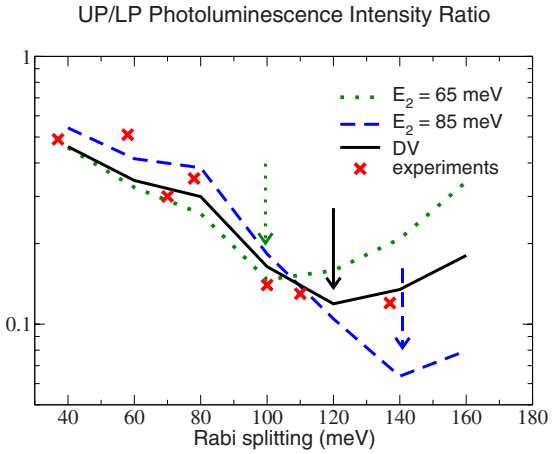

FIG. 4. (Color online) C ratio as function of the Rabi splitting for microcavities with $\beta=0$, for the DV model ($E_2=75$ meV) in continuous line, with E_2 changed in 65 meV (dotted line) and with $E_2=85$ meV (dashed line). The calculation is compared with the experimental data in "x's" (Ref. 20).

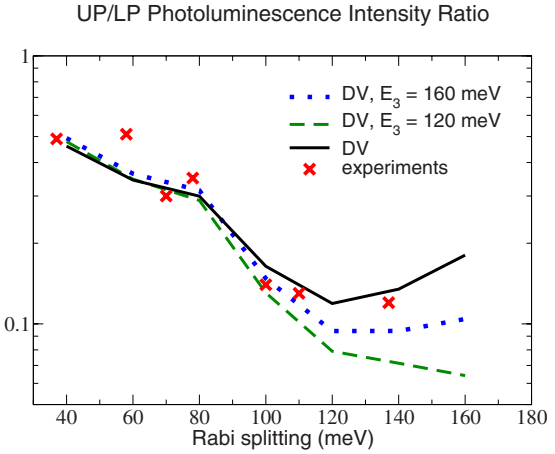

FIG. 6. (Color online) C ratio as function of the Rabi splitting for microcavities with $\beta=0$, for the DV model plus a high-energy vibration $E_3=120$ (dotted) and 160 meV (dashed). The calculation is compared with the experimental data in "x's" (Ref. 20).

tion $E_0=5$ meV instead of the continuous spectrum of low-energy vibrations. The result in Fig. 5 is a significant reduction in the C factor for Δ smaller than 120 meV. We can understand this if we consider that UP population is mainly due to the ER to UP scattering that takes place from steady-state ER population with absorption of a molecular vibration, while the direct relaxation in UP from high-energy excitons gives a minor contribution. This process involving absorption of vibrations is active at room temperature until around $E_0=K_bT$ (if the vibrational DOS is not zero); therefore it is significant for UP energies equal to the mean ER population energy (ε) plus k_bT that corresponds to Rabi splitting values $\Delta<2(\varepsilon+K_bT)\approx 80$ meV. Therefore a reduction in the active low-energy DOS means a significant reduction in the ER to UP scattering and of the C ratio for small Δ. If we modify

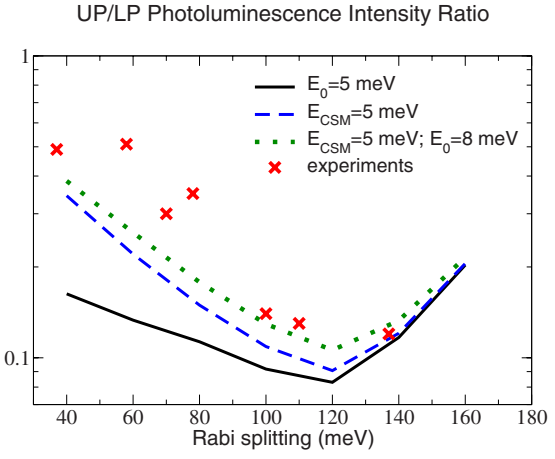

FIG. 5. (Color online) C ratio as function of the Rabi splitting for microcavities with $\beta=0$ and low-energy vibrational spectrum modified with respect to the DV model. Simulation with no CSV and a defined energy vibration $E_0=5$ meV (continuous line); with $E_{CSM}=5$ meV (dashed); with $E_{CSM}=5$ meV, plus a defined energy vibration $E_0=8$ meV (dotted). The calculation is compared with the experimental data in "x's" (Ref. 20).

DV choosing $E_{CSM}=5$ meV, we note that after $\Delta=2(\varepsilon+E_{CSM})=40$ meV we have a rapid decrease in the C factor and a minimum, as predicted around 120 meV. So it is clear that to recover the experimental data, we need a series of active vibrations between 5 and 25 meV.

Finally let us consider the effects of a third optical vibration $E_3>E_2$, in particular, we set $E_3=120$ meV or $E_3=160$ meV with $g_3=0.3$. As can be seen in Fig. 6 the presence of E_3 has effects on C only for large enough Rabi splitting, for which $\Delta/2+\varepsilon$ approaches E_3. For $E_3=120$ meV, with Δ in the range considered, the nonmonotonic behavior of C vanishes correspondent to the fact that the LP is pumped from the ER almost thermalized population with an emission of a vibration E_3. If we increase E_3 to 160 meV, the ER to LP scattering becomes too much out of resonance to contribute and numerical data are nearer to the DV case. It must be noted that the possible presence of a C minimum is conditioned to the absence of optical vibrations of higher energy E_3 active in relaxation processes.

IV. CONCLUSIONS

In conclusion our model based on semiclassical rate equations explains sufficiently well the presently available experimental data on strongly coupled J-aggregate microcavities. In particular, the photoluminescence under nonresonant pumping follows the scattering of an electronic excitation from the ER bottom, where the population is accumulated, toward the polariton branches. Such scattering can either happen with the absorption/emission of vibrational quanta (with a continuous as well as discrete spectrum), process which is sensitive to temperature, or be due to pumping of polaritons by the spontaneous radiative decay of weakly coupled excitons. The interplay between the two processes determines both the specific temperature dependence of the polariton branches photoluminescence intensity ratio and its Rabi splitting dependence.

*michetti@df.unipi.it

[1] *The Physics of Semiconductor Microcavities*, edited by B. Deveaud (Wiley, Weinheim, 2007).
[2] M. Saba, C. Ciuti, J. Bloch, V. Thierry-Mieg, R. Andre, L. S. Dang, S. Kundermann, A. Mura, G. Bongiovanni, J. L. Staehli, and B. Deveaud, Nature (London) **414**, 731 (2001).
[3] J. Kasprzak, M. Richard, S. Kundermann, A. Baas, P. Jeambrun, J. M. J. Keeling, F. M. Marchetti, M. H. Szymanska, R. Andre, J. L. Staehli, V. Savona, P. B. Littlewood, B. Deveaud, and Le Si Dang, Nature (London) **443**, 409 (2006).
[4] D. G. Lidzey, D. D. C. Bradley, M. S. Skolnick, T. Virgili, S. Walker, and D. M. Whittaker, Nature (London) **395**, 53 (1998).
[5] P. A. Hobson, W. L. Barnes, D. G. Lidzey, G. A. Gehring, D. M. Whittaker, M. S. Skolnick, and S. Walker, Appl. Phys. Lett. **81**, 3519 (2002).
[6] D. G. Lidzey, D. D. C. Bradley, T. Virgili, A. Armitage, M. S. Skolnick, and S. Walker, Phys. Rev. Lett. **82**, 3316 (1999).
[7] J. R. Tischler, M. S. Bradley, V. Bulovic, J. H. Song, and A. Nurmikko, Phys. Rev. Lett. **95**, 036401 (2005).
[8] R. J. Holmes and S. R. Forrest, Phys. Rev. Lett. **93**, 186404 (2004).
[9] L. Fontanesi and G. C. La Rocca, Phys. Status Solidi C **5**, 2441 (2008).
[10] R. J. Holmes and S. R. Forrest, Org. Electron. **8**, 77 (2007).
[11] D. G. Lidzey, in *Electronic Excitations in Organic Based Nanostructures: Thin Films and Nanostructures*, edited by V. M. Agranovich and F. Bassani (Elsevier, San Diego, 2003), Vol. 31, Chap. 8.
[12] V. M. Agranovich, M. Litinskaia, and D. G. Lidzey, Phys. Rev. B **67**, 085311 (2003).
[13] P. Michetti and G. C. La Rocca, Phys. Rev. B **71**, 115320 (2005).
[14] V. M. Agranovich and Y. N. Gartstein, Phys. Rev. B **75**, 075302 (2007).
[15] P. Michetti and G. C. La Rocca, Physica E **40**, 1926 (2008).
[16] M. Litinskaya, P. Reineker, and V. M. Agranovich, J. Lumin. **119-120**, 277 (2006).
[17] P. Michetti and G. C. La Rocca, Phys. Rev. B **77**, 195301 (2008).
[18] H. Zoubi and G. C. La Rocca, Phys. Rev. B **71**, 235316 (2005).
[19] H. Zoubi and G. C. La Rocca, Phys. Rev. B **72**, 125306 (2005).
[20] J. Chovan, I. E. Perakis, S. Ceccarelli, and D. G. Lidzey, Phys. Rev. B **78**, 045320 (2008).
[21] P. Michetti and G. C. La Rocca, http://dx.doi.org/10.1002/pssc.200880310
[22] D. G. Lidzey, A. M. Fox, M. D. Rahn, M. S. Skolnick, V. M. Agranovich, and S. Walker, Phys. Rev. B **65**, 195312 (2002).
[23] *J-Aggregates*, edited by T. Kobayashi (World Scientific, Singapore, 1996).
[24] M. Bednarz, V. A. Malyshev, and J. Knoester, J. Chem. Phys. **117**, 6200 (2002).
[25] D. J. Heijs, V. A. Malyshev, and J. Knoester, J. Chem. Phys. **123**, 144507 (2005).
[26] S. Ceccarelli, J. Wenus, M. S. Skolnick, and D. G. Lidzey, Superlattices Microstruct. **41**, 289 (2007).
[27] P. Schouwink, J. M. Lupton, H. von Berlepsch, L. Dahne, and R. F. Mahrt, Phys. Rev. B **66**, 081203(R) (2002).
[28] D. Embriaco, D. B. Balagurov, G. C. La Rocca, and V. M. Agranovich, Phys. Status Solidi C **1**, 1429 (2004).
[29] A. L. Ivanov and L. V. Keldysh, Sov. Phys. JETP **57**, 234 (1982); B. S. Wang and J. L. Birman, Phys. Rev. B **42**, 9609 (1990).